Atomic arrangement in the mSnTe-nBi_2Te_3 compounds by electronic structure calculations

1991 J. Phys.: Condens. Matter 3 1461

(http://iopscience.iop.org/0953-8984/3/11/008)

J. Phys.: Condens. Matter 3 (1991) 1461–1474. Printed in the UK

Atomic arrangement in the mSnTe–nBi$_2$Te$_3$ compounds by electronic structure calculations

F Casula, L Deiana and A Podda

Istituto di Fisica, University of Cagliari, Via della Pineta 77, I-09125 Cagliari, Italy and
Consorzio INFM, Unita' di Cagliari, Italy

Received 4 June 1990, in final form 8 November 1990

Abstract. mA^{IV}Te–nB$_2^V$Te$_3$ systems form well-defined compounds, characterized by a layer structure, where the Te planes are intercalated by the metallic ones. Both ordered and random distributions of A and B atoms in the cation sites have been invoked by the experimentalists. The different possible sequences of filled and unfilled sandwiches of Te planes might induce additional disorder in the unit cell when $n > 1$.

Our calculations for such a system, specifically for mSnTe–nBi$_2$Te$_3$, based on a tight-binding effective Hamiltonian, give a clear indication in favour of ordered structures. This would explain why these systems do not form solid solutions. The results for the sequence of Te and metallic planes suggest SnBi$_2$Te$_4$ to be the only stable compound in the system, the others quoted in the literature being just combinations of that unit cell with the Bi$_2$Te$_3$ cell.

1. Introduction

mA^{IV}Te–nB$_2^V$Te$_3$ (A = Sn, Ge, Pb; B = Sb, Bi) systems present layer structures, where the atoms are octahedrally coordinated, in a manner very similar to the Bi$_2$Te$_3$ structure [1]. In addition the Te planes, also in these compounds, form a sort of host matrix, whose octahedral cavities are ordinarily filled by metallic atoms, but for stoichiometric reasons some Te planes have to face one another directly. The existence of these unfilled Te sandwiches produces a relaxation in the corresponding layers, which makes inequivalent the local environments of the different Te atoms of the basis and causes a distortion of the adjacent filled cavities. Recently interest has been focused on this point, because examination of the x-ray and Mössbauer spectra led to different conclusions as to the distribution of metal atoms in the cation sites of mSnTe–nBi$_2$Te$_3$ systems. In fact a random distribution of metal atoms both in the distorted and undistorted octahedral cavities was invoked as the one which would give highest accordance between the theoretical and experimental results for x-ray spectra [2]. On the other hand the absence of splitting in the Mössbauer peak—and of any linewidth enlargement with respect to the SnTe data—calls for a regular distribution of the Mössbauer-active Sn atoms in the undistorted cavities only [3]. In the following we will use the terms disorder and order with reference to these two atomic arrangements in the crystal cell.

In this context electronic energy calculations can help in solving the dilemma and can give useful suggestions to the experimentalists. Hence preliminary results on

0953-8984/91/111461+14$03.50

$SnBi_2Te_4$, i.e. the 50/50 combination of SnTe and Bi_2Te_3, have already been published [4] and these favoured the ordered distribution of cations. In this paper we will examine the problem more thoroughly, by also studying the $SnBi_4Te_7$, i.e. the $(n = 1, m = 2)$ system, and the $Sn_2Bi_6Te_{11}$, i.e. the $(n = 2, m = 3)$ system. These compounds, together with $Sn_5Bi_{12}Te_{23}$, are all those actually prepared and experimentally studied in the mSnTe–$n$$Bi_2Te_3$ family [2, 3]. The exclusion of $Sn_5Bi_{12}Te_{23}$, which will save computer time, can be accepted because the experimental situation is very similar for all the compounds of the family, so that we can easily extend our conclusions to it. We stress that these systems, as well as the more general $mA^{IV}Te$–$nB_2^VTe_3$ ones, do not form solid solutions between the cubic and the hexagonal parent compound, but only well-defined compounds [1–3]. This experimental finding will be explained later.

The study of the more complicated $SnBi_4Te_7$ and $Sn_2Bi_6Te_{11}$ structures led us to face the problem of the correct sequence of filled and unfilled Te sandwiches in the unit cell. We recall that the $mA^{IV}Te$–$nB_2^VTe_3$ compound crystal structure can be described by an hexagonal cell, with a basis resulting from three packets of $2m + 5n$ atoms in different layers, or by a rhombohedral cell, with just one $2m+5n$ atom packet in the basis [1]. In AB_4Te_7 one packet already contains a layer number multiple of three and therefore it is also a sufficient basis for the hexagonal cell. Clearly the three packets in the hexagonal cell do not differ for the sequence of Te and metal layers, but for the atomic arrangement on the corresponding layers. Now let us observe that in the single $SnBi_2Te_4$ packet we have four Te layers and therefore three Te sandwiches to be filled by the three metallic layers, the unfilled sandwiches being confined to the inter-packet space (packet borders are marked by Te layers). This is not the case for $SnBi_4Te_7$ and $Sn_2Bi_6Te_{11}$, where six and ten intra-packet Te sandwiches can only be filled by five and eight metallic layers respectively. We have therefore also investigated the correct sequence for filled and unfilled sandwiches in the cell in order to determine the one corresponding to the most stable crystal structure. In section 2 we will briefly outline the theoretical method, whilst sections 3 and 4 will be devoted to the results of $SnBi_4Te_7$ and $Sn_2Bi_6Te_{11}$ respectively. The conclusions will be drawn in section 5.

2. Theoretical method

In this paper we want to study the electronic energy levels of crystals with a large number of atoms in the cell, each of which has different possible atomic arrangements. We need, therefore, a method whose results we can rely on, but which we can use extensively for all the compounds and structures of the family. Moreover the experimental results available up until now have been more of a chemical or crystallographic nature than accurate measurements directly comparable with energy levels. Thus we adopt a localized Wannier-like representation for the electronic orbitals, with a minimal s and p basis set. We assume an effective Hamiltonian, which includes only first-neighbour interactions, and whose matrix elements have been fitted from SnTe and Bi_2Te_3 results. For the theoretical grounds of localized methods in energy-band calculations and for an extensive review on the field, we refer the reader to [5] and [6], while applications of a similar method have recently proved successful for, e.g. SnTe [7], $SnBi_2Te_4$ [4] and even for a metal such as Al [8].

The transferability of interaction parameters from the parent compounds SnTe and Bi_2Te_3 to the crystals under study is granted by the persistence for each basis atom of the same first neighbours at almost the same distances as can be seen in table 1 of [4].

The table is devoted to $SnBi_2Te_4$, but can be extended to $SnBi_4Te_7$ and $Sn_2Bi_6Te_{11}$. Since we are using effective interactions, it is also important that second neighbours, and qualitatively the whole atomic environment, do not change this much, as in fact, they do.

Clearly we cannot guarantee that this method will reproduce the 'exact' density of states (in the following simply indicated as DOS for the sake of brevity) for the chosen arrangement of atoms in the unit cell. However, such theoretical results must undergo some broadening in order to be compared, say, with photoemission spectra. Thus we will reach one of our goals if DOS plots corresponding to different atomic arrangements still show, after a reasonable broadening, significant differences between them. While the possibility of attributing one of our theoretical DOS to the actual layer sequence in the crystal is postponed until the availability of these kinds of experimental data, other global estimates on the stability of different arrangements will be presented in section 5. Again, we will obtain for different layer sequences large enough energy differences to give us confidence in the validity of the conclusion we will draw, even though the numerical results could be altered by different choices of input parameters or by the adoption of other theoretical approaches.

Actual values of parameters used in determining the effective Hamiltonian matrix elements are reported in [9]. They have been partly deduced from [7] and partly obtained by fitting the energy levels of [10]. In addition the exclusion of relativistic effects in treating bismuth atoms can be largely justified because of the independence of our conclusions from fine details in the band structure, as previously discussed. As a matter of fact our non-relativistic results for the Bi_2Te_3 DOS, after a Gaussian broadening [11], and recent relativistic calculations [13] for the same material give results of comparable quality in the interpretation of the photoemission data [12].

Since we are not specifying the exact form of the localized functions in our basis, we cannot obtain the explicit expression of either the crystal electronic eigenfunctions or the charge distribution. However, we still have access to fundamental information about our systems, i.e. the DOS

$$n(E) = \int_\Omega \mathrm{d}^3k \, \Sigma_j \delta[E - E_j(\boldsymbol{k})]$$

and also its analysis in terms of partial local densities of states (PLDOS)

$$n_{i,l}(E) = N_i^{-1} \int_\Omega \mathrm{d}^3k \, \Sigma_j w_{j,i,l}(\boldsymbol{k}) \delta[E - E_j(\boldsymbol{k})]$$

where $l = s, p$ refers to the wavefunction angular character and i numbers the inequivalent crystal sites, each one corresponding to N_i basis atoms in the cell. The energy eigenvalues $E_j(\boldsymbol{k})$ and the weight $w_{j,i,l}(\boldsymbol{k})$ of the (i, l) basis functions in the jth eigenstate are obtained by diagonalizing the full effective Hamiltonian matrix. Integrals over the Brillouin zone Ω are performed by means of the tetrahedron method [13]. One hundred $\boldsymbol{k}$-points in the irreducible wedge of Ω have been used for the $SnBi_4Te_7$ calculations, whilst for $Sn_2Bi_6Te_{11}$, where 228×228 matrices are diagonalized, we used only 32 $\boldsymbol{k}$-points. A test calculation for comparing 100 and 32 $\boldsymbol{k}$-point DOS revealed differences of less than 4%, with no alteration in the form and position of peaks [21].

Moreover, by the reasonable assumption that the basis functions are strongly localized, we can estimate the numbers of s or p electrons around the ith site:

$$z_{i,l} = \int_0^{E_F} \mathrm{d}E \, n_{i,l}(E)$$

where the integral is performed up to the Fermi energy E_F. For what attains to total energies, we can easily calculate the band structure contributions

$$E_{bs} = \int_0^{E_F} dE\, E\, n(E)$$

whilst a correct calculation of the electrostatic contributions E_{es}, or at least of their differences, would imply knowledge of the electronic charge densities [5]. As a matter of fact, despite its name, E_{es} is not reducible to the Coulombic energy E_{mad} of an ionic point charge system. Nevertheless the variations in E_{mad}, which can be easily computed by means of the Ewald technique [15], after taking into account the actual screening of valence electrons $z_{i,l}$ on the core charges, will be useful in determining the stability of different structures.

We are aware that nowadays there are much more sophisticated methods for computing electronic energies in crystals from first principles, even for ternary compounds [16]. However, to the best of our knowledge the largest cells which have been studied by means of these methods include up to 14 atoms, compared with the 57 we used in the $Sn_2Bi_6Te_{11}$ calculations. Moreover we do not know of any first-principle calculation, which includes such heavy atoms as bismuth. Finally we do not think that, at least for a long while, 'exact' calculations will completely rule out 'approximate' calculations similar to those previously described. Instead they could be very usefully coupled together whenever a lengthy investigation over a series of compounds has to be done and the reliability of the results has to be checked in some test cases.

3. $SnBi_4Te_7$ electronic structures

In the literature there is some uncertainty about the cell of $SnBi_4Te_7$, which on the basis of the x-ray analysis was claimed to be similar to that of $SnBi_2Te_4$, with twelve Te and nine metal layers, whose sites should statistically be unoccupied in order to reproduce the chemical formula [2]. Similar conclusions for the analogous $PbBi_4Te_7$ results [17] were later revised after new electron diffraction data [18] on that system became available. It was possible to attribute to the $PbBi_4Te_7$ cell a structure based on seven Te and five metal layers, as in $GeBi_4Te_7$, and to explain the x-ray results through the reaction

$$2PbBi_4Te_7 \rightarrow Pb_2Bi_2Te_5 + 3Bi_2Te_3$$

which leaves in the annealed sample, after evaporation of the volatile Bi_2Te_3, a mixture of $PbBi_4Te_7$ and $Pb_2Bi_2Te_5$ with 21 layers [19]. We cannot advance such a solution for $SnBi_4Te_7$ without new crystallographic data, but it is hard to admit a statistical distribution of occupied and unoccupied hexagonal sites on the layers of a system which does not even like to form solid solutions and, as we shall see, prefers an ordered arrangement of atoms.

We adopt for $SnBi_4Te_7$ the more reasonable $PbBi_4Te_7$ and $GeBi_4Te_7$ structure. In the unit cell there are six octahedral cavities to be filled with only five metallic ions; one cavity inside the cell will remain unfilled. It can be placed in the first, second or third Te sandwich and we will accordingly call the three resulting atomic arrangements

$SnBi_4Te_7$-1, $SnBi_4Te_7$-2, $SnBi_4Te_7$-3. Schematically the three-layer sequences are:

$SnBi_4Te_7$-1: Te2–Te2–Bi–Te1–Bi–Te1–Sn–Te1–Bi–Te1–Bi–Te2

$SnBi_4Te_7$-2: Te2–Bi–Te2–Te2–Bi–Te1–Bi–Te1–Sn–Te1– Bi–Te2

$SnBi_4Te_7$-3: Te2–Bi–Te1–Bi–Te2–Te2–Bi–Te1–Sn–Te1–Bi–Te2

The other possibilities, i.e. the unfilled cavity in the fourth, fifth or sixth sandwich, are equivalent to the third, second and first one, respectively. Note that for the time being we are not including any disorder of the metal atoms, but we had to make a distinction, already present in Bi_2Te_3, between relaxed (Te2) and unrelaxed (Te1) layers, which mark the boundaries of the unfilled and filled sandwiches, respectively.

The DOS corresponding to these three sequences are shown in figure 1. Before discussing our findings, we stress that, in the absence of specific experimental results on electronic properties, we did not attempt a fine adjustment of the interaction parameters, our purpose being to establish some general trends. In all of the three cases the crystal appears to be a zero-gap semiconductor, in reasonable agreement with the electrical measurements, which indicate a degenerate semiconductor [20]. However, marked differences in the DOS are apparent and persist even after a peak broadening [17], so that they should be appraised by a photoemission study. Going to a finer examination, we can look at the PLDOS, reported in figures 2 and 3. We are showing only the Sn- and Te2-centred PLDOS in order to illustrate two different situations: an unchanged first- and second-neighbour environment for the Sn atoms and a modified neighbour arrangement for Te2 atoms. In fact Sn PLDOS show only minor variations in comparison with those present in Te2 PLDOS. This examination helps clarify some specific points: e.g. the two highest peaks, one at −6.0 eV in the $SnBi_4Te_7$-1 DOS and the other at −3.4 eV in the $SnBi_4Te_7^{-2}$ DOS, are not only shifted, but also have different characters, i.e. s and p, respectively, as can be seen in figure 3. Again these differences should be detected by careful photoemission studies.

In order to examine the differences between an ordered and disordered distribution of cations on the metallic layers we present two DOS in figure 4, both of which correspond to the $SnBi_4Te_7$-3 sequence of filled and unfilled Te sandwiches

$SnBi_4Te_7$-3: Te2–Me2–Te1–Me2–Te2–Te2–Me2–Te1–Me1–Te1–Me2–Te2.

In the ordered arrangement the Me1 sites are occupied by Sn atoms and the Me2 ones by Bi atoms, whilst in the fully disordered arrangement Sn and Bi atoms are randomly distributed on metallic sites according to their stoichiometric ratio. Disorder is simulated through the virtual crystal approximation (VCA) The two DOS do not differ very much, this being different from the analogous results for $SnBi_2Te_4$ [4]. In fact the overall contribution of metallic atoms to the DOS in the ordered arrangement is already dominated by the Bi contribution so that the disorder-induced VCA mixing of interaction parameters—in the ratio 1:4, to be compared with the ratio 1:2 of $SnBi_2Te_4$—produces only minor changes. As expected, the modifications are much more appreciable in the PLDOS for the Me1 site, as shown in figure 5.

4. $Sn_2Bi_6Te_{11}$ electronic stuctures

There is no detailed information in the literature on the crystal structure of $Sn_2Bi_6Te_{11}$, but it has been prepared and characterized as a single-phase crystal [3].

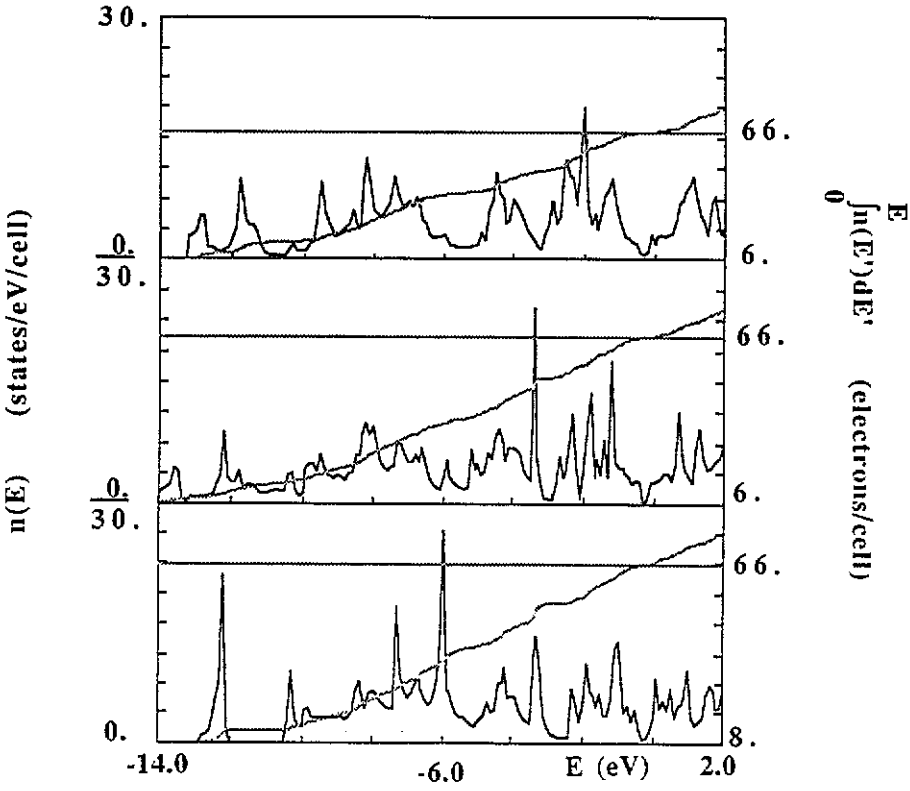

Figure 1. Density of states (full lines) for the three conceivable layer sequences in $SnBi_4Te_7$: from the bottom $SnBi_4Te_7$-1, $SnBi_4Te_7$-2 and $SnBi_4Te_7$-3. The integrated DOS and the cell electron number (lighter lines) are also plotted against the energy E: their intersection point gives the Fermi energy value. The scales on the left refer to the DOS, the ones on the right to the integrated DOS.

We assume, therefore, the typical layer structure for these compounds with the same interatomic distances as in $SnBi_2Te_4$. We adopt the 57 layer hexagonal unit cell, thus also obtaining a test of the potentiality of the method. Again we have, in a packet, ten Te sandwiches to be filled with eight metallic layers. The 45 ways of choosing the positions of the two unfilled sandwiches in the full sequence can be reduced to 25 by symmetry, but unfortunately for each one we have many different possibilities for alternating the Bi and Sn layers, whilst still keeping the ordered character of the crystal. Since we cannot present detailed results for all of them, we consider here only three highly symmetric sequences as being those in which we could expect the smallest differences to appear.

In figure 6 we present the resulting DOS for these three-layer sequences:

$Sn_2Bi_6Te_{11}$-4.7: Te2–Bi–Te1–Sn–Te1–Bi–Te2–Te2–Bi–
Te1–Bi–Te2–Te2–Bi–Te1–Sn–Te1–Bi–Te2

$Sn_2Bi_6Te_{11}$-2.9: Te2–Bi–Te2–Te2–Bi–Te1–Sn–Te1–Bi–
Te1–Bi–Te1–Sn–Te1–Bi–Te2–Te2–Bi–Te2

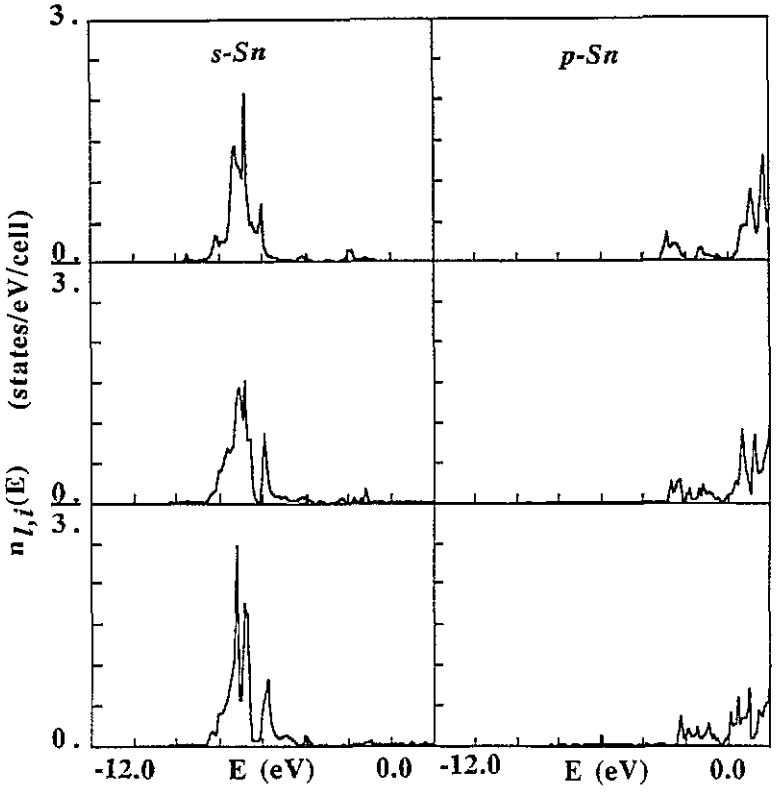

Figure 2. The PLDOS for s (left) and the p (right) states on Sn: from the bottom $SnBi_4Te_7$-1, $SnBi_4Te_7$-2 and $SnBi_4Te_7$-3.

$Sn_2Bi_6Te_{11}$-1.10: Te2–Te2–Bi–Te1–Bi–Te1–Sn–Te1–Bi–
Te1–Bi–Te1–Sn–Te1–Bi–Te1–Bi–Te2–Te2

where the notations 4.7, 2.9 and 1.10 refer to the positions of the unfilled sandwiches. Results for many more layer arrangements are reported in [21]. We note that, despite the similar symmetric arrangement that characterizes the three structures, the results are quite different. In particular, in the two upper DOS the peaks appear to be quite uniformly distributed, whilst in the $Sn_2Bi_6Te_{11}$-4.7 DOS the peaks are well separated. This gives rise after broadening to markedly different structures, which could easily be compared with experimental photoemission results. It generally turns out that, among the $Sn_2Bi_6Te_{11}$ structures we examined, the '4.7' one produces the neatest DOS [21].

In figure 7 we compare, for the previously mentioned atomic arrangements, the p PLDOS on Sn and Te2, which are responsible for the behaviour around the Fermi energy and for the disappearance of the small gap in $Sn_2Bi_6Te_{11}$-2.9 and $Sn_2Bi_6Te_{11}$-1.10. $Sn_2Bi_6Te_{11}$ is expected, by analogy with the other compounds in the family, to be a small-gap semiconductor. However, the problem is not the non-zero DOS at the Fermi energy, which could be eliminated by a fine readjustment of the interaction parameters, but the disappearance of the valley around the Fermi energy.

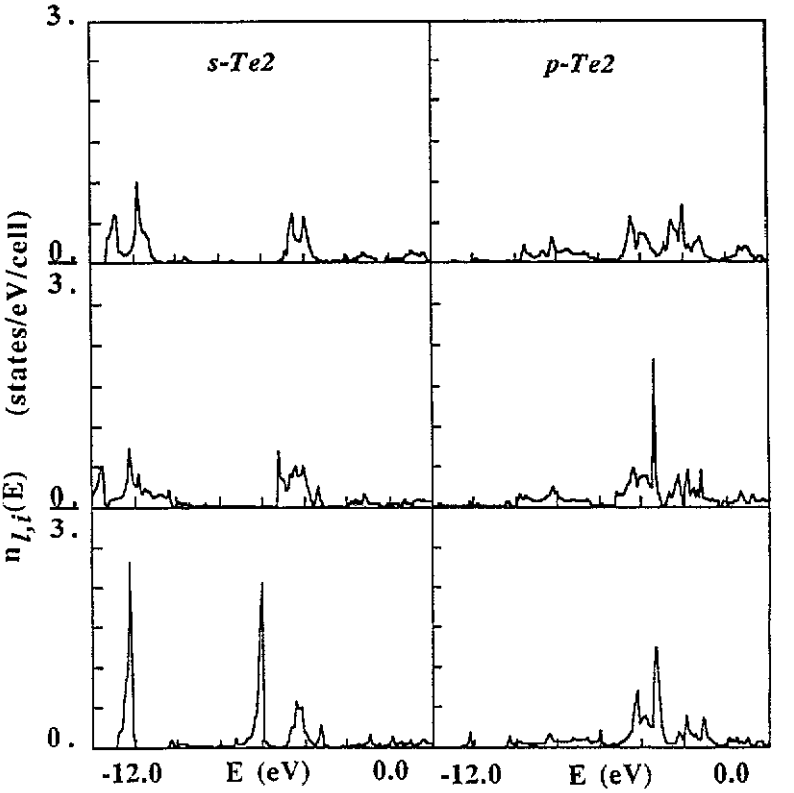

Figure 3. The PLDOS for s (left) and p (right) states on Te2: from the bottom $SnBi_4Te_7$-1, $SnBi_4Te_7$-2 and $SnBi_4Te_7$-3.

Finally in figure 8 we present the effect on the DOS of the ordered or random distribution of metal atoms in the sequence

$Sn_{22}Bi_6Te_{11}$-4.7: Te2–Me2–Te1–Me1–Te1–Me2–Te2–Te2–Me2–
Te1–Me2–Te2–Te2–Me2–Te1–Me1–Te1–Me2–Te2.

As we pointed out before, since the Sn and Bi atoms are in the ratio 1:3, the modifications induced by disorder are more easily detectable than in $SnBi_4Te_7$, even for the total DOS.

5. Discussion and conclusions

Let us now discuss briefly how our results can be compared with experiment in the absence of photoemission data. We start with the alternative between ordered and disordered arrangement, which has been examined in [2] and [3]. Mössbauer analysis is able to estimate the number of p valence electrons on Sn $p_{Sn,exp}$ applying a widely used empirical formula [22]. For all the compounds of the mSnTe–$n$$Bi_2Te_3$ family, because of the almost identical values of the measured isomer shift, $p_{Sn,exp} \simeq 0.64$ [3].

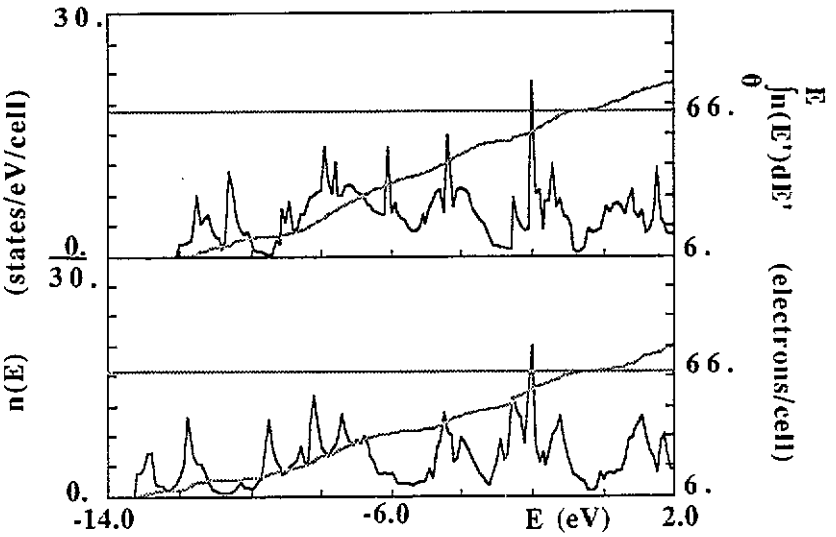

Figure 4. The DOS of $SnBi_4Te_7$-3 with an ordered (bottom) or a fully disordered (top) arrangement of cations on metal layers. As in figure 1 the lighter lines and the scales on the right refer to the integrated DOS and the total electron number.

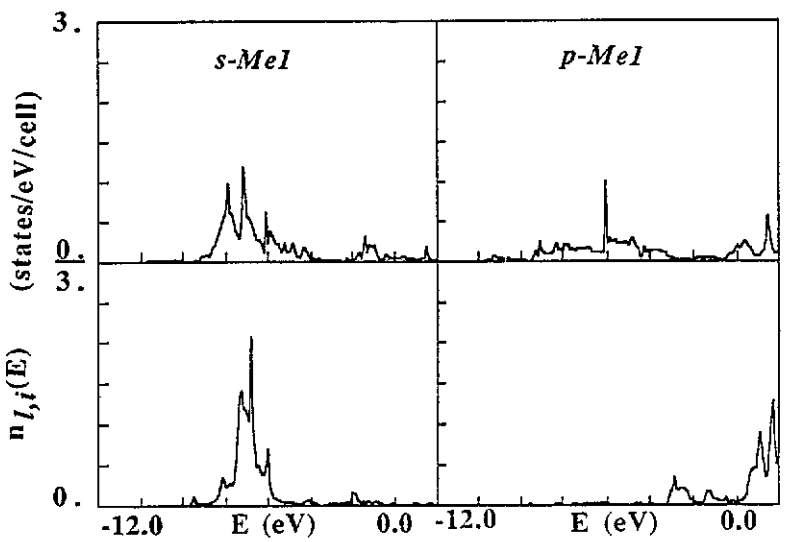

Figure 5. PLDOS for s (left) and p (right) states on Me1 site of $SnBi_4Te_7$-3: from the bottom ordered and fully disordered arrangement of cations on metal layers.

We can compare this result with $z_{Sn,p}$ for the ordered arrangement. Unfortunately in a hypothetical disordered arrangement the Mössbauer experiment would select only the Sn contribution—it does not matter where the atom would be placed—whilst the calculated values of $z_{Me1,p}$ and $z_{Me2,p}$ contain a contribution from both a Sn and a Bi

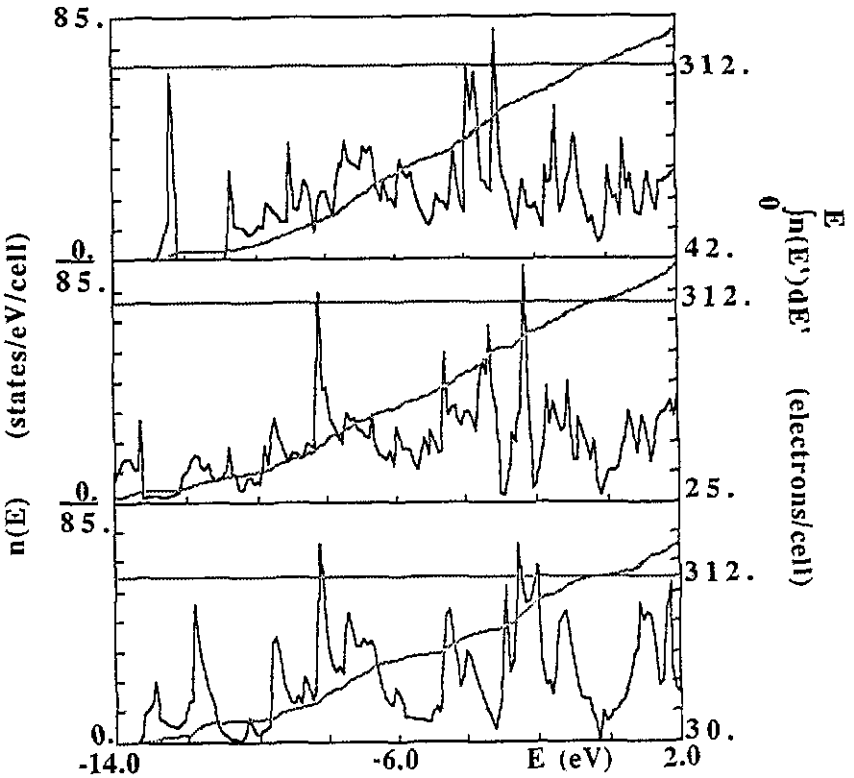

Figure 6. The DOS (full lines), integrated DOS and the cell electron number (lighter lines) for three layer sequences in $Sn_2Bi_6Te_{11}$: from the bottom $Sn_2Bi_6Te_{11}$-4.7, $Sn_2Bi_6Te_{11}$-2.9, $Sn_2Bi_6Te_{11}$-1.10. The scales on the left refer to the DOS, the ones on the right to the integrated DOS.

atom. In the framework of a VCA calculation, we can reasonably accept the following formulae

$$z_{\mathrm{Me1,p}} = x_{1,\mathrm{Sn}} z_{1,\mathrm{p,Sn}} + (1 - x_{1,\mathrm{Sn}}) z_{1,\mathrm{p,Bi}}$$

$$z_{\mathrm{Me2,p}} = x_{2,\mathrm{Sn}} z_{2,\mathrm{p,Sn}} + (1 - x_{2,\mathrm{Sn}}) z_{2,\mathrm{p,Bi}}$$

where $x_{i,\mathrm{Sn}}$ and $z_{i,\mathrm{p,Sn}}$ ($z_{i,\mathrm{p,Bi}}$) are the percentage of Sn atoms and the Sn (Bi) p valence electron number on Me1 ($i = 1$) or Me2 ($i = 2$) sites. Assuming $z_{1,\mathrm{p,Sn}}$ and $z_{2,p,Bi}$ to be the same in the ordered and disordered arrangement, because of the unchanged local environment, we can also obtain a rough estimate for the 'disordered' values of $z_{2,\mathrm{p,Sn}}$ and therefore of

$$p_{\mathrm{Sn,th}} = x_{1,\mathrm{Sn}} z_{1,\mathrm{p,Sn}} + x_{2,\mathrm{Sn}} z_{2,\mathrm{p,Sn}}$$

which is the value to be compared with $p_{\mathrm{Sn,exp}}$. The results are shown in table 1. We remark that both the choice of a first-neighbour effective Hamiltonian and the VCA approximation are expected to underestimate the changes produced by disorder in the

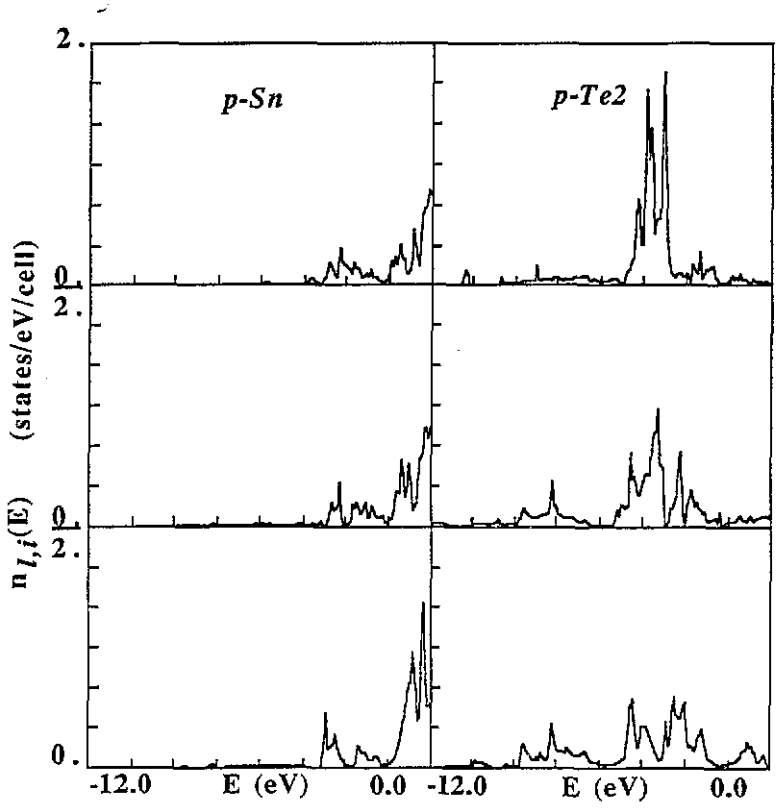

Figure 7. The PLDOS for p states on Sn (left) and p states on Te2 (right): from the bottom $Sn_2Bi_6Te_{11}$-4.7, $Sn_2Bi_6Te_{11}$-2.9, $Sn_2Bi_6Te_{11}$-1.10.

electronic properties and therefore the substantial divergence of the 'disordered' value of $p_{Sn,th}$ from the experimental estimate $p_{Sn,exp}$ is a reliable indication in favour of the ordered arrangement.

Let us now examine the results given in table 2 in order to determine which sequence of filled and unfilled Te sandwiches produces the most stable structure. For the layer sequences in $SnBi_4Te_7$ and $Sn_2Bi_6Te_{11}$ the total ionic charges Z_i (i = Sn, Bi, Te1, Te2), as they result after atomic cores have been screened by valence electrons localized on each crystal site, are given in table 2. These point charge systems give rise to Madelung-like energies E_{Mad}, which are also reported in the table and are compared with the total band structure energies, E_{bs}. We have already stated that our method cannot produce accurate numerical values of E_{tot}, and we have not even attempted to estimate them by summing E_{bs} and E_{Mad}. On the other hand the E_{Mad} variations are so marked with respect to the slight differences in E_{bs}, that they should play a fundamental role in determining the stability of the proposed structures.

We remark that such large variations in E_{Mad} are not due to extremely high values of ionic charges, nor to their large percentage variations, but essentially to different geometries. In order to prove this last point we computed E_{Mad} in the hypothetical situations where the effective atomic charges of $SnBi_4Te_7$-3 are attributed to atoms arranged in the $SnBi_4Te_7$-1 and in the $SnBi_4Te_7$-2 layer sequences and similarly the

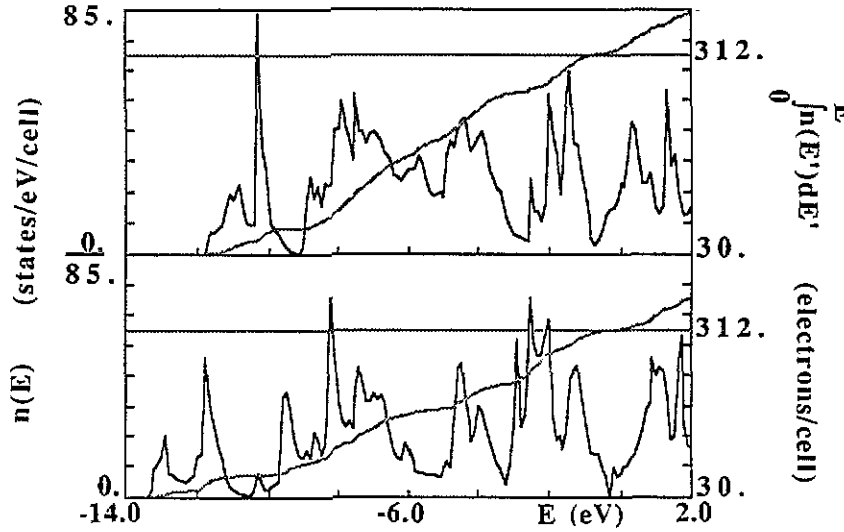

Figure 8. The DOS of $Sn_2Bi_6Te_{11}$-4.7 with an ordered (bottom) or a fully disordered (top) arrangement of cations on metal layers. As in figure 1 the lighter lines and the scales on the right refer to the integrated DOS and the total electron number.

effective charges of $Sn_2Bi_6Te_{11}$-4.7 are attributed to atoms arranged in the other $Sn_2Bi_6Te_{11}$ layer sequences. For the former sequences E_{Mad} passes, respectively, from 146.6 to 73.04 eV and from 91.08 to 82.28 eV, while for $Sn_2Bi_6Te_{11}$-2.9 and $Sn_2Bi_6Te_{11}$-1.10 it passes, respectively, from 921.96 to 932.6 eV and from 2253.37 to 1014.4 eV. In a way, these large E_{Mad} values indicate that the atoms do not like to be forced into the corresponding unit cell arrangement no matter which ionic charges are sitting on them. On the other hand E_{bs}, based on a short-range Hamiltonian, does not show any relevant variations for different layer sequences.

Table 1. Comparison of the values obtained for the p valence electron number on Sn atoms in the ordered and disordered arrangements of $SnBi_2Te_4$, $SnBi_4Te_7$ and $Sn_2Bi_6Te_{11}$. Values marked † have been assumed to be the same in both arrangements. See the text for explanation of the symbols. Experimental values from [3].

	$SnBi_2Te_4$		$SnBi_4Te_7$		$Sn_2Bi_6Te_{11}$	
	ord	disord	ord	disord	ord	disord
$x_{1,Sn}$	1	0.333	1	0.20	1	0.25
$x_{2,Sn}$	0	0.666	0	0.80	0	0.75
$z_{Me1,p}$	1.04	3.25	1.03	3.48	1.02	3.41
$z_{Me2,p}$	3.55	3.00	3.54	3.24	3.58	3.17
$z_{1,p,Sn}$	1.04	1.04†	1.03	1.03†	1.02	1.02†
$z_{2,p,Bi}$	3.55	3.55†	3.54	3.54†	3.58	3.58†
$z_{2,p,Sn}$		1.90		2.04		1.94
$p_{Sn,th}$	1.04	1.61	1.03	1.84	1.02	1.71
$p_{Sn,exp}$	0.64		0.65		0.64	

$SnBi_4Te_7$-3 and $Sn_2Bi_6Te_{11}$-4.7 clearly appear to be the most stable geometries for the corresponding chemical composition. Further results for different arrangements of $Sn_2Bi_6Te_{11}$,reported in [21], confirm this conclusion. We stress that these stable

Table 2. Total (nuclear plus electronic) ionic charges (in +e units) Z_i on non-equivalent crystal sites (i = Sn, Bi, Te1, Te2), obtained through band structure calculations and used in computation of the Coulombic energy E_{Mad} for the three geometries of $SnBi_4Te_7$ and for three typical geometries of $Sn_2Bi_6Te_{11}$. The total band energies E_{bs} are also displayed. All energy values are in eV.

		Z_{Sn}	Z_{Bi}	Z_{Te1}	Z_{Te2}	E_{Mad}	E_{bs}
	-1	0.92	−0.50	1.02	−1.00	146.60	−481.64
$SnBi_4Te_7$	-2	0.98	−0.36	0.89	−0.54	91.08	−475.51
	-3	1.00	−0.34	0.80	−0.52	36.68	−475.03
	-4.7	1.01	−0.37	0.73	−0.57	217.73	−2223.17
$Sn_2Bi_6Te_{11}$	-2.9	0.91	−0.38	0.77	−0.56	921.96	−2225.23
	-1.10	0.85	−0.58	0.98	−1.27	2253.37	−2266.26

structures are obtained by combining, as building blocks, the $SnBi_2Te_4$ and the Bi_2Te_3 packets. This is the reason for the almost identical values for the Sn-based measurements in all the compounds of the mSnTe–$n$$Bi_2Te_3$ system. In a way such a marked preference for this crystal architecture is the reason for inhibiting any kind of disorder in the metallic sublattice. In turn the requirement for an ordered structure calls for fixed proportions of Sn and Bi atoms and does not allow the formation of solid solutions. These conclusions enlighten, even though qualitatively, similar experimental results for the whole $mA^{IV}Te$–$nB_2^{V}Te_3$ family [1, 2].

We think that two main points can be stressed as conclusions:

(i) we have obtained a reasonable picture of the properties of the mSnTe–$n$$Bi_2$–$Te_3$, specifically the formation of well-defined compounds and the absence of disorder in the cation sublattice; detailed results for DOS and PLDOS are available for comparison with any forthcoming photoemission data;

(ii) we have proved the usefulness of such tight-binding effective Hamiltonians in obtaining reliable results with an affordable computational time, whenever a full range of compositions and crystal structures have to be investigated; some test first-principle calculations on selected compounds would be advisable for further confirmation of this point.

Acknowledgments

Many valuable discussions with Professor G Mula at various stages of this work are gratefully acknowledged. The authors are also indebted to Professors F Ledda and C Muntoni for enlightening reports on the properties of these materials. This work has been supported by Italian National Research Council (CNR) through 'Progetto Finalizzato Sistemi Informatici a Calcolo Parallelo' under Grant No. 89-00006-69.

References

[1] Hulliger F 1976 *Structural Chemistry of Layer-Type Phases* vol 5 (Dordrecht: Reidel)
[2] Zhukova B and Zaslavskii A I 1972 *Sov. Phys. Crystallogr.* **16** 796
[3] Ledda F, Muntoni C, Serci S and Pellerito L 1987 *Chem. Phys. Lett.* **134** 545
[4] Casula F, Deiana L, Ledda F, Mula G and Muntoni C 1987 *Ternary and Multinary Compounds* (Pittsburgh: MRS) p 543

[5] Heine V 1980 *Solid State Physics* **35** (New York: Academic) p 1
[6] Bullett D W 1980 *Solid State Physics* **35** (New York: Academic) p 129
[7] Polatoglou H M, Theodorou G and Economou N A 1986 *Phys. Rev.* B **33** 1265
[8] Casula F, Andreoni W and Maschke K 1986 *J. Phys. C: Solid State Phys.* **19** 5155
[9] Deiana L 1987 *Thesis* University of Cagliari (in Italian)
[10] Borghese F and Donato C 1968 *Nuovo Cimento* B **53** 283
[11] Casula F and Deiana L 1987 unpublished (internal report)
[12] Pecheur P and Toussaint G 1989 *Phys. Lett.* **135** 223
[13] Thuler M R, Benbow R L and Hurych Z 1982 *Chem. Phys.* **71** 265
[14] Skriver H L 1984 *The LMTO Method* (Berlin: Springer) p 194
[15] Ewald P P 1921 *Ann. Phys.* **64** 253
[16] Marinelli M, Baroni S and Meloni F 1988 *Phys. Rev.* B **38** 8258
Massidda S, Continenza A, Freeman A J, de Pascale T M, Meloni F and Serra M 1990 *Phys. Rev.* B **41** 12079 and references therein
[17] Talybov A G and Vainshtein B K 1962 *Sov. Phys. Crystallogr.* **6** 432
[18] Petrov I I and Imamov R M 1970 *Sov. Phys. Crystallogr.* **14** 593
[19] Vainshtein B K, Imamov M and Talybov A G 1970 *Sov. Phys. Crystallogr.* **14** 596
[20] Tichy L, Frumar M, Kincl K, Klikorka J and Tryska A 1981 *Phys. Stat. Sol.* a **6** 461
[21] Podda A 1989 *Thesis* University of Cagliari (in Italian)
[22] Lees J and Flinn P A 1965 *Phys. Lett.* **19** 186